

Separation of a Slater determinant wave function with a neck structure into spatially localized subsystems

Yasutaka TANIGUCHI¹ and Yoshiko KANADA-EN'YO²

¹*RIKEN Nishina Center for Accelerator-Based Science, RIKEN, Wako, Saitama 351-0109, Japan.*

²*Department of Physics, Kyoto University, Kyoto, Kyoto 606-8502, Japan.*

A method to separate a Slater determinant wave function with a two-center neck structure into spatially localized subsystems is proposed, and its potential applications are presented. An orthonormal set of spatially localized single-particle wave functions is obtained by diagonalizing the coordinate operator for the major axis of a necked system. Using the localized single-particle wave functions, the wave function of each subsystem is defined. Therefore, defined subsystem wave functions are used to obtain density distributions and mass centers of subsystems. The present method is applied to the separation of Margenau–Brink cluster wave functions of $\alpha + \alpha$, $^{16}\text{O} + ^{16}\text{O}$, and $\alpha + ^{16}\text{O}$ into their subsystems, and also to the separation of antisymmetrized molecular dynamics wave functions of ^{10}Be into $\alpha + ^6\text{He}$ subsystems. The method is simple and can be applied to the separation of general Slater determinant wave functions that have neck structures into subsystem wave functions.

§1. Introduction

Nuclear systems often exhibit multi-center structures having spatially localized subsystems, as seen in phenomena such as cluster structures and the fusion/fission process. In cluster structures, each system consists of more than one spatially localized subsystems, called clusters, and intercluster motion is a degree of freedom used to describe the structure of a total system. In such multi-center systems, constituent nucleons of each cluster and the internuclear distance are useful parameters to specify cluster features. Identification of subsystems is also important for nuclear reactions, in which colliding nuclei are subsystems. In order to have an in-depth understanding of nuclear systems with subsystems, wave functions of each subsystem should be defined microscopically.

For microscopic wave functions of quantum fermion systems, the Slater determinant description is often adopted as used in the Hartree–Fock (HF) and the time-dependent HF (TDHF) approaches, the Brink–Bloch model, and the antisymmetrized molecular dynamics (AMD) method.^{1)–3)} Many applications to studies of nuclear structures and reactions show that two-center structures have localized subsystems. However, a method to microscopically separate a Slater determinant into subsystem wave functions is not obvious, particularly when subsystems overlap with each other. One of the popular ways to separate the density of a total system into those of subsystems is to employ the method of sharp-cut density separated by a boundary plane. However, the sharp-cut density is based on a classical picture and it is a nonphysical entity in quantum systems because density distributions have singularities at the boundary plane. In the cases of Margenau–Brink (MB)⁴⁾ wave functions (which are used in the Brink–Bloch model) and AMD wave functions, sub-

system wave functions can be broadly defined as cluster wave functions or groups of single-particle Gaussian wave packets. However, the subsystem wave functions in the overlapping region of two clusters contain nonphysical components that vanish because of the Pauli blocking effect, that is, antisymmetrization of nucleons in the total wave function.

The aim of this paper is to propose a method to define wave functions of spatially localized subsystems in a Slater determinant wave function. With this method, a total system is microscopically separated into subsystems. Applications to $N = Z$ nuclei, ^8Be ($\alpha + \alpha$), ^{32}S ($^{16}\text{O} + ^{16}\text{O}$), ^{20}Ne ($\alpha + ^{16}\text{O}$), and $N \neq Z$ nucleus, ^{10}Be ($\alpha + ^6\text{He}$) are shown. We compared the internuclear distances defined by the present method with those from sharp-cut density and single-particle Gaussian centroids of AMD wave functions.

In §2, we propose a method to define wave functions of subsystems. In §3, the method is applied to MB wave functions for $Z = N$ systems and AMD wave functions of ^{10}Be , and the density distributions of subsystems and internuclear distance are shown. In §4, characteristics of the method are discussed. Finally, conclusions are given in §5.

§2. Framework

Suppose a Slater determinant wave function $|\Phi\rangle$ having two-center structures as

$$|\Phi\rangle = \hat{\mathcal{A}}|\tilde{\varphi}_1, \tilde{\varphi}_2, \dots, \tilde{\varphi}_A\rangle, \quad (2.1)$$

where $\hat{\mathcal{A}}$ is the antisymmetrization operator, A is the mass number of a total system, and $\tilde{\varphi}_1, \dots, \tilde{\varphi}_A$ are single-particle wave functions. Here, the z axis is chosen to be the major axis of the total system. Note that the total wave function $|\Phi\rangle$ is invariant except for the normalization under any linear transformations of single-particle wave functions $\{\tilde{\varphi}_i\} \rightarrow \{\varphi_i\}$, which gives nonzero determinants.

In order to separate the total system into two subsystems I and II, subsystem wave functions are defined as follows: First, single-particle wave functions are transformed in order to diagonalize norm and coordinate operators \hat{z} ,

$$|\varphi_i\rangle = \sum_j |\tilde{\varphi}_j\rangle c_{ji}, \quad (2.2)$$

$$\langle \varphi_i | \varphi_j \rangle = \delta_{ij}, \quad (2.3)$$

$$\langle \varphi_i | \hat{z} | \varphi_j \rangle = z_i \delta_{ij}, \quad (2.4)$$

where $z_1 \leq z_2 \leq \dots \leq z_A$. The eigenvalue z_i indicates the mean position of the i th nucleon. If a single-particle wave function φ_i is localized at a certain position, z_i can be regarded as the nucleon position in a semi-classical picture. Therefore, it is natural to classify φ_i into two groups $\{\varphi_1, \varphi_2, \dots, \varphi_{A_1}\}$ and $\{\varphi_{A_1+1}, \varphi_2, \dots, \varphi_A\}$ according to the distribution of z_i . Here, A_1 and $A_2 \equiv A - A_1$ are regarded as the number of nucleons constituting subsystems I and II, respectively.

Once single-particle wave functions are separated, the internuclear distance and expected values of any operators (such as the density distribution for each subsystem)

can be calculated. The mass centers \mathbf{R}_I and \mathbf{R}_{II} of subsystems I and II are obtained as

$$\mathbf{R}_I = \frac{1}{A_1} \sum_{i=1, \dots, A_1} \langle \varphi_i | \hat{\mathbf{r}} | \varphi_i \rangle, \quad (2.5)$$

$$\mathbf{R}_{II} = \frac{1}{A_2} \sum_{i=A_1+1, \dots, A} \langle \varphi_i | \hat{\mathbf{r}} | \varphi_i \rangle, \quad (2.6)$$

respectively. Then, the internuclear distance R is defined as the distance between the mass centers,

$$R = |\mathbf{R}_{II} - \mathbf{R}_I|. \quad (2.7)$$

Density distributions $\rho_I(\mathbf{r})$ and $\rho_{II}(\mathbf{r})$ of subsystems I and II are calculated by

$$\rho_I(\mathbf{r}) = \sum_{i=1, \dots, A_1} \rho_i(\mathbf{r}), \quad (2.8)$$

$$\rho_{II}(\mathbf{r}) = \sum_{i=A_1+1, \dots, A} \rho_i(\mathbf{r}), \quad (2.9)$$

respectively. Here, $\rho_i(\mathbf{r})$ is the density distribution of the i -th nucleon,

$$\rho_i(\mathbf{r}) = \langle \varphi_i | \delta(\hat{\mathbf{r}} - \mathbf{r}) | \varphi_i \rangle. \quad (2.10)$$

§3. Results

3.1. $N = Z$ nuclei

In this section, the current separation method is applied to the MB wave functions. In the MB wave function for a system consisting of two clusters, clusters I and II are expressed by the shell-model configurations with centers at $(0, 0, -\frac{A_2}{A}d)$ and $(0, 0, +\frac{A_1}{A}d)$, respectively. The parameter d specifies the degree of cluster development. MB wave functions for two-cluster systems, $\alpha + \alpha$, $\alpha + {}^{16}\text{O}$, and ${}^{16}\text{O} + {}^{16}\text{O}$ are considered, and subsystem density distributions and internuclear distances are calculated by the present method.

3.1.1. ${}^8\text{Be}$ ($\alpha + \alpha$)

In an MB wave function $|\Phi_{\alpha+\alpha}\rangle$ with an $\alpha + \alpha$ cluster structure, the α clusters I and II are expressed by the $(0s)^4$ shell model wave function shifted to the positions $-d/2$ and $d/2$, respectively, as

$$|\Phi_{\alpha+\alpha}\rangle = \hat{\mathcal{A}}|\tilde{\varphi}_1, \tilde{\varphi}_2, \dots, \tilde{\varphi}_8\rangle, \quad (3.1)$$

$$|\tilde{\varphi}_{1,5}\rangle = |\tilde{\phi}_{1,2} \otimes p \uparrow\rangle, \quad (3.2)$$

$$|\tilde{\varphi}_{2,6}\rangle = |\tilde{\phi}_{1,2} \otimes p \downarrow\rangle, \quad (3.3)$$

$$|\tilde{\varphi}_{3,7}\rangle = |\tilde{\phi}_{1,2} \otimes n \uparrow\rangle, \quad (3.4)$$

$$|\tilde{\varphi}_{4,8}\rangle = |\tilde{\phi}_{1,2} \otimes n \downarrow\rangle, \quad (3.5)$$

$$\langle \mathbf{r} | \tilde{\phi}_{1,2} \rangle = \left(\frac{2\nu}{\pi} \right)^{\frac{3}{4}} e^{-\nu(\mathbf{r} \pm \frac{\mathbf{d}}{2})^2}, \quad (3.6)$$

where the $\mathbf{d} = (0, 0, d)$, p and n are a proton and neutron, respectively, the \uparrow and \downarrow indicate up and down spins, respectively, and the ν indicates the width of Gaussian wave packets. In the large d limit, the antisymmetrization effect is small enough and the mean position of α clusters I and II are $\mp \mathbf{d}/2$, respectively. Therefore, in a semi-classical picture, the parameter d is regarded as the internuclear distance. However, when the spatial parts ϕ_1 and ϕ_2 have a non-negligible overlap with each other, d does not represent the internuclear distance because the single-particle wave functions in the overlapping region are modified by the Pauli blocking effect.

The transformation given by Eq. (2.1)–(2.4) obtains analytical forms of spatially localized single-particle wave functions in the $\alpha + \alpha$ system as

$$|\varphi_{1,5}\rangle = |\phi_{1,2} \otimes p \uparrow\rangle, \quad (3.7)$$

$$|\varphi_{2,6}\rangle = |\phi_{1,2} \otimes p \downarrow\rangle, \quad (3.8)$$

$$|\varphi_{3,7}\rangle = |\phi_{1,2} \otimes n \uparrow\rangle, \quad (3.9)$$

$$|\varphi_{4,8}\rangle = |\phi_{1,2} \otimes n \downarrow\rangle, \quad (3.10)$$

$$\langle \mathbf{r} | \phi_{1,2} \rangle = c_+ e^{-\nu(\mathbf{r} \pm \frac{\mathbf{d}}{2})^2} + c_- e^{-\nu(\mathbf{r} \mp \frac{\mathbf{d}}{2})^2}, \quad (3.11)$$

$$c_{\pm} = \frac{1}{2} \left(\frac{2\nu}{\pi} \right)^{\frac{3}{4}} \left(\sqrt{\frac{1 - e^{-\frac{1}{2}\nu d^2}}{1 - e^{-\nu d^2}}} \pm \sqrt{\frac{1 + e^{-\frac{1}{2}\nu d^2}}{1 - e^{-\nu d^2}}} \right). \quad (3.12)$$

Eigen values $\{z_i\}$ of \hat{z} are

$$z_{1,2,3,4} = -\frac{d}{2\sqrt{1 - e^{-\nu d^2}}}, \quad (3.13)$$

$$z_{5,6,7,8} = +\frac{d}{2\sqrt{1 - e^{-\nu d^2}}}, \quad (3.14)$$

which are scaled by $1/\sqrt{1 - e^{-\nu d^2}}$ when compared to the positions of centroids of wave packets $\mp \mathbf{d}$. The internuclear distance R between α clusters is, therefore,

$$R = \frac{d}{\sqrt{1 - e^{-\nu d^2}}}. \quad (3.15)$$

The internuclear distance R tends to $\nu^{-1/2}$ in the $d \rightarrow 0$ limit.

Figure 1 shows the spatial parts of the spatially localized single-particle wave functions $\phi_{1,2}$ as well as Gaussian wave packets $\tilde{\phi}_{1,2}$ at $d = 4, 2$, and $1 \nu^{-1/2}$, and the $d \rightarrow 0$ limit. In the case of $d = 4 \nu^{-1/2}$, ϕ_i almost coincides with $\tilde{\phi}_i$, whereas ϕ_i has an obvious node in the $d \leq 2\nu^{-1/2}$ region where $\tilde{\phi}_1$ and $\tilde{\phi}_2$ overlap. The wave functions ϕ_1 and ϕ_2 are spatially localized even for $d \rightarrow 0$.

Figure 2 shows linear density distributions $\rho_{xy\text{I,II}}(z)$ of α clusters I and II defined by the integrated subsystem densities with respect to x and y ,

$$\rho_{xy\text{I,II}}(z) = \iint dx dy \rho_{\text{I,II}}(\mathbf{r}). \quad (3.16)$$

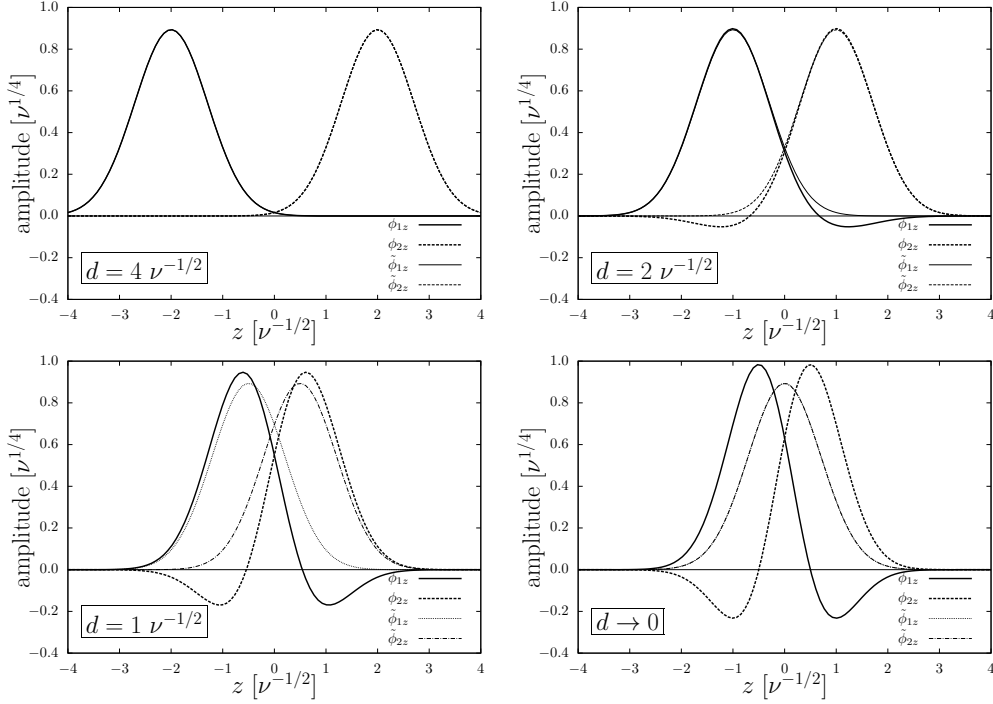


Fig. 1. Amplitudes of a z -part of single-particle wave functions ϕ_1 (solid) and ϕ_2 (dashed), where a z -part of ϕ_i is defined as $\phi_i / \left[(2\nu/\pi)^{1/2} e^{-\nu(x^2+y^2)} \right]$, in $\alpha + \alpha$ MB wave functions are plotted with the parameters $d = 4$ (upper left), 2 (upper right), and $1 \nu^{-1/2}$ (lower left), while $d \rightarrow 0$ (lower right) are plotted as functions of z . The Gaussian wave packets for the original single particle wave functions $\tilde{\phi}_{1,2z}$ (dotted and dot-dashed, respectively) before antisymmetrization are also shown. Units of the amplitudes and z are in $\nu^{1/4}$ and $\nu^{-1/2}$, respectively.

Density distributions of four single-particle wave functions in each cluster are the same because of spin and isospin saturation. Unlike the sharp-cut separation, subsystem densities are always smooth. Density distributions of α clusters I and II are spatially localized, even in the case of $d \rightarrow 0$.

Figure 3 shows internuclear distances R by the present method and R_ρ obtained by the sharp-cut separation as functions of distance parameter d between the centroids of wave packets. R_ρ is calculated analytically as

$$R_\rho = \frac{1}{\sqrt{2\pi\nu}} \frac{1}{\sinh(\frac{1}{2}\nu d^2)} \left[\sum_{n=0}^{\infty} \frac{n! (2\nu d^2)^n}{(2n)!} - e^{-\frac{1}{2}\nu d^2} \right]. \quad (3.17)$$

In $d \gtrsim 2 \nu^{-1/2}$, R and R_ρ are similar and they are close to d . In $d \lesssim 2 \nu^{-1/2}$, where α clusters overlap with each other, R is smaller than R_ρ .

3.1.2. ^{20}Ne ($\alpha + ^{16}\text{O}$)

Figure 4 shows linear density distributions for the α and ^{16}O clusters, as well as spatially localized single-particle orbits of α and ^{16}O clusters in $\alpha + ^{16}\text{O}$ MB wave functions with $d = 8, 4, 2$, and 1 fm. Width parameters ν are set to 0.16 fm^{-2} .

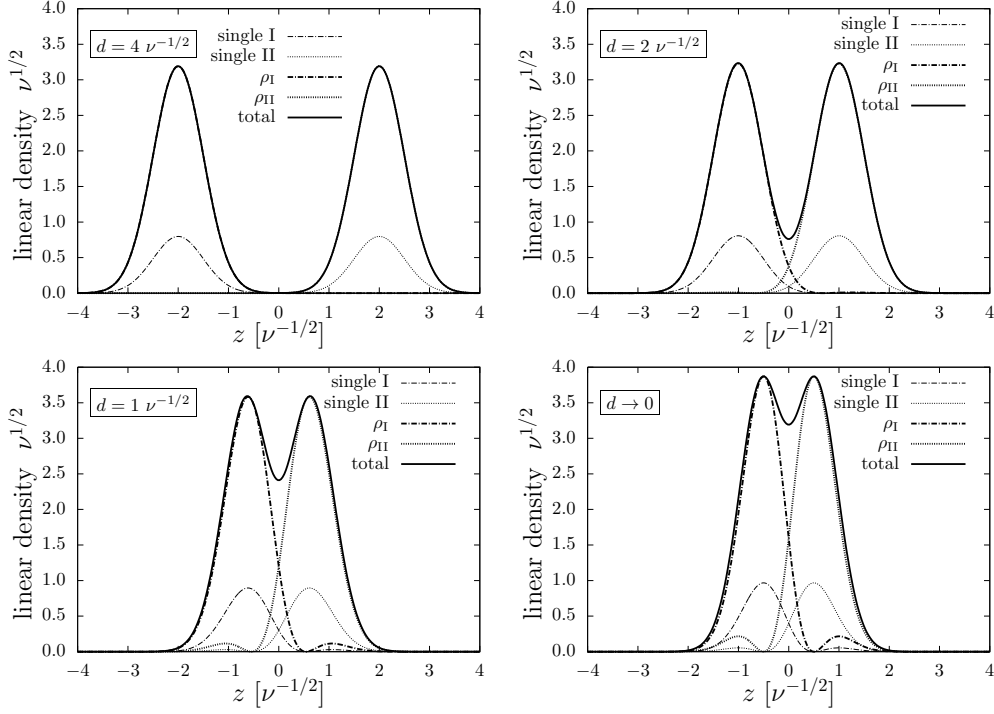


Fig. 2. Linear density distributions of α clusters I and II, spatially localized single-particle wave functions, and the total system in $\alpha + \alpha$ MB wave functions with the parameter $d = 4$ (upper left), 2 (upper right), $1 \nu^{-1/2}$ (lower left), and $d \rightarrow 0$ (lower right) are plotted as functions of z . Thin dot-dashed and dotted lines represent single-particle wave functions for α clusters I and II, respectively. Thick dot-dashed and dotted lines represent α clusters I and II, respectively. Solid lines represent total wave functions. Units of linear densities and z are in $\nu^{1/2}$ and $\nu^{-1/2}$, respectively.

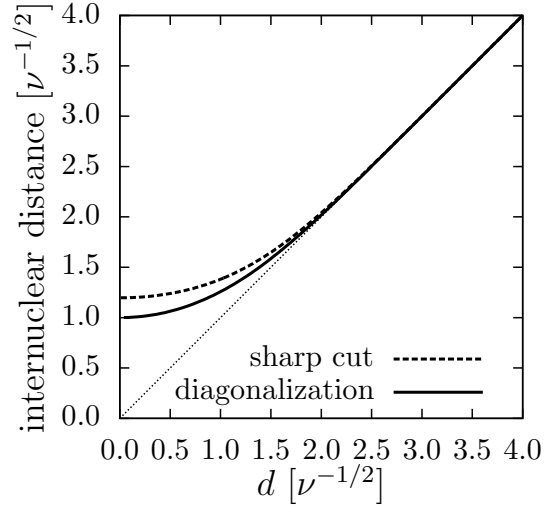


Fig. 3. Internuclear distance is defined by the present method (solid) and sharp-cut separation (dashed) as functions of distance between centroids of wave packets in units of $\nu^{-1/2}$.

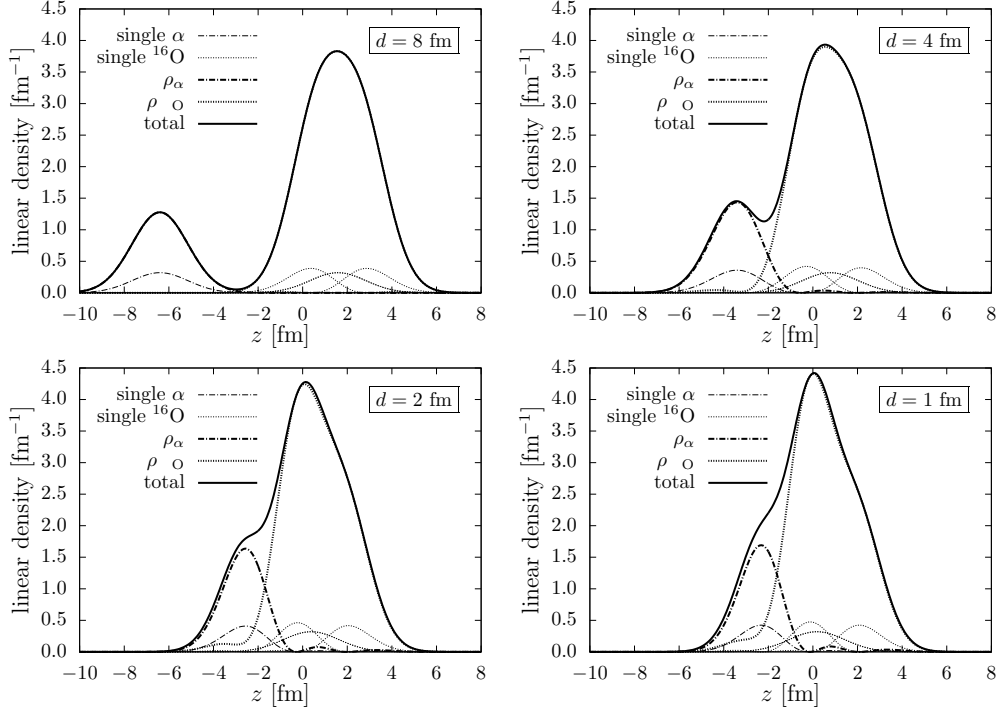


Fig. 4. Linear density distributions of α and ^{16}O clusters and that for the total system in the $\alpha+^{16}\text{O}$ MB wave functions with the parameter $d = 8, 4, 2$, and 1 fm. Thin dot-dashed and dotted lines represent single-particle wave functions for α and ^{16}O clusters, respectively. Thick dot-dashed and dotted lines represent α and ^{16}O clusters, respectively. Solid lines represent total wave functions. Units of linear densities and z are fm^{-1} and fm , respectively.

At the small d region, α and ^{16}O clusters have nodes in the overlap region because of antisymmetrization effects between clusters, but they are still spatially localized. Subsystem densities have no singularity.

Figure 5 shows the internuclear distance R and R_ρ between α and ^{16}O clusters defined by the present method and sharp-cut separation, respectively. R is smaller than R_ρ in the $d \lesssim 6$ fm region, and they are similar in the $d \gtrsim 6$ fm region.

3.1.3. ^{32}S ($^{16}\text{O}+^{16}\text{O}$)

Figure 6 shows linear density distributions of ^{16}O clusters and spatially localized single-particle wave functions in $^{16}\text{O} + ^{16}\text{O}$ MB wave functions with $d = 10, 6, 5$, and 2 fm. Each total density distribution shows an interesting neck between two clusters, and each single-particle wave function is well localized. Therefore, nucleons are separated into two ^{16}O clusters. The densities of the total system and the two ^{16}O clusters are also shown in the figure. In the touching region such as $d = 5$ and 6 fm, the density profile for each ^{16}O cluster defined in the present method also shows reasonable shapes. Subsystem densities have no singularity, and are smoothly damped in the overlap region.

The internuclear distance R determined by the present method is plotted as a

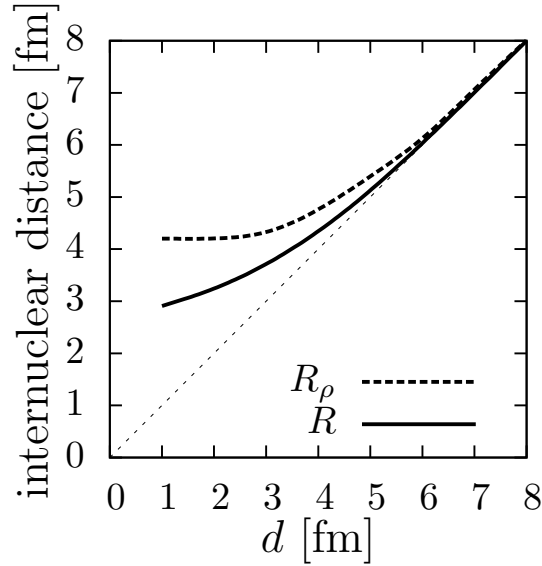


Fig. 5. Internuclear distance between α and ^{16}O clusters is defined by the present method (solid) and sharp-cut separation (dashed) as functions of distance between centroids of wave packets. Units are fm.

function of d in Fig. 7. The distance R_ρ defined by the sharp-cut density is also shown for comparison. R equals to d in the large d region, and as d decreases, it deviates from d toward the $R > d$ region. In the $d = 0$ limit also, the internuclear distance R has a finite value because of the Pauli blocking effect. The behavior of R is qualitatively similar to that of R_ρ . However, quantitatively, R is slightly smaller than R_ρ because the left and right nuclei have an overlap density in the present definition instead of the sharp-cut density.

3.2. $N \neq Z$: ^{10}Be ($\alpha + ^6\text{He}$)

In this section, the present method is applied to AMD wave functions for $N \neq Z$ nucleus ^{10}Be that is calculated by energy variations after parity and angular momentum projection.⁵⁾ In the AMD model, an intrinsic wave function is expressed by Slater determinants of single-particle wave functions each of which is written by a Gaussian wave packet. Gaussian centers of all nucleons are treated as independently varying parameters, and therefore, no clusters are assumed. One of the advantages of the AMD method is that the formation and/or breaking of clusters can be described in the framework. Since clusters are not assumed in the AMD model, a grouping of nucleons into two clusters is not necessarily obvious, unlike the MB cluster model wave functions.

Analyzing the mean position z_i of nucleons determined by the present method, single-particle wave functions φ_i can be separated into two subsystems I and II. Four nucleons have z_i in the left of the neck position and form an α cluster (subsystem I). Six nucleons having z_i in the right of the neck can be classified in subsystem II corresponding to a ^6He cluster. Figure 8 shows linear density distributions of

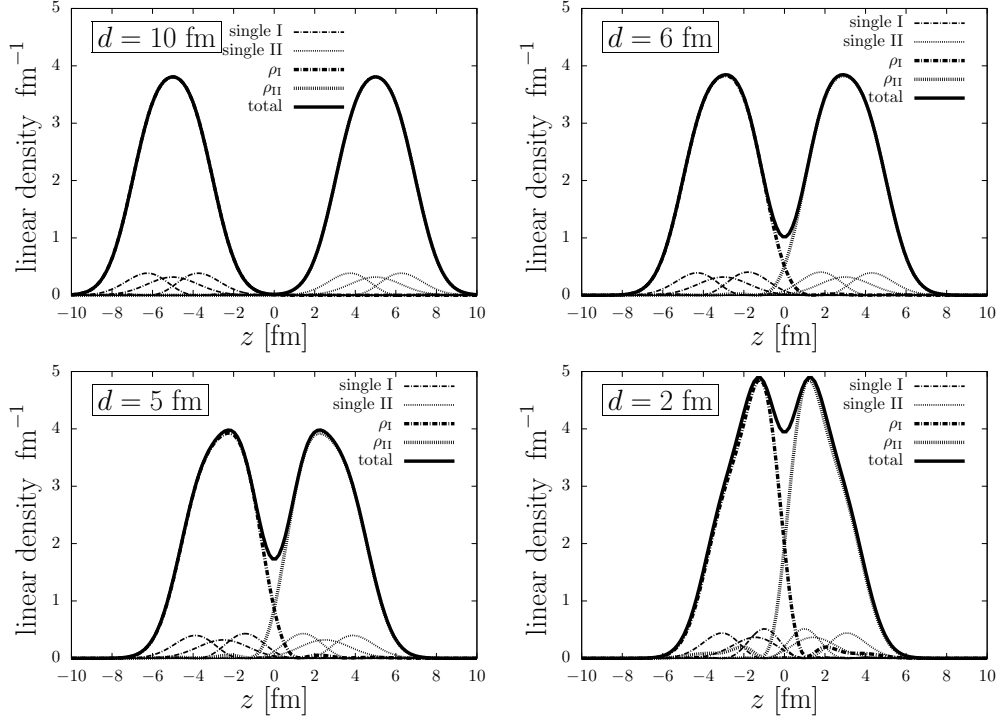


Fig. 6. Linear density distributions of ^{16}O clusters I and II, and the total system in $^{16}\text{O}+^{16}\text{O}$ MB wave functions with the parameter $d = 10, 6, 5$, and 2 fm are plotted as functions of z . Thick dot-dashed and dotted lines represent single-particle wave functions for ^{16}O clusters I and II, respectively. Thin dot-dashed and dotted lines represent ^{16}O clusters I and II, respectively. Solid lines represent the total wave functions. Units of linear densities and z are in fm^{-1} and fm.

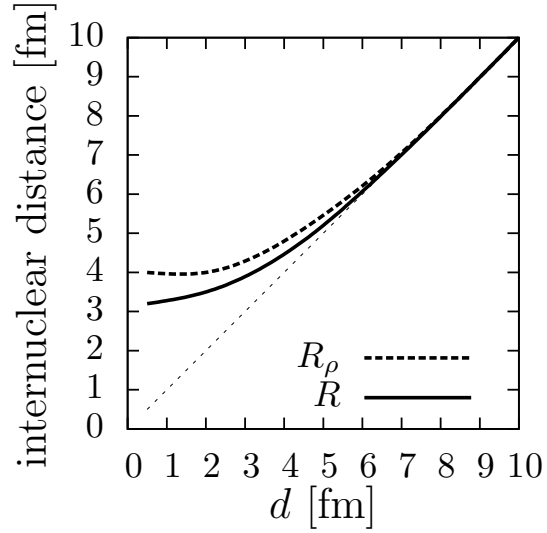


Fig. 7. Internuclear distance between ^{16}O clusters is defined by the present method (solid) and sharp-cut separation (dashed) as functions of the distance between centroids of wave packets. Units are fm.

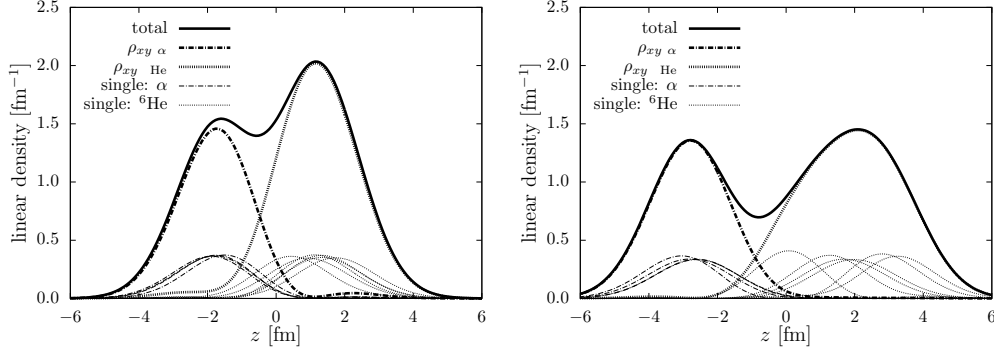


Fig. 8. Linear density distributions of intrinsic wave functions of dominant components of the $J^\pi = 0_1^+$ (left) and 0_2^+ (right) states in ^{10}Be . Thin dot-dashed and dotted lines represent single-particle wave functions for α and ^6He clusters, respectively. Thick dot-dashed and dotted lines represent α and ^6He clusters, respectively. Solid lines represent total wave functions. Units of linear densities and z are in fm^{-1} and fm .

dominant components of the $J^\pi = 0_1^+$ and 0_2^+ states in ^{10}Be , which are separated into α and ^6He clusters. In both states, total linear density distributions have necks at $z \sim 0$ fm, and single-particle orbits localize left and right parts. Therefore, the entire ^{10}Be system can be separated into two clusters using the present separation method.

§4. Discussions

The previous section shows that the present separation method involving the diagonalization of a spatial operator of the major axis works well for the separation of a Slater determinant wave function into spatially localized wave functions of subsystems. The results of applications to MB wave functions with $\alpha + \alpha$, $\alpha + ^{16}\text{O}$, and $^{16}\text{O} + ^{16}\text{O}$ structures are shown in Figs 2, 4, and 6, respectively. With this method, we obtained subsystem wave functions with no singularities. This is one of the advantages over the sharp-cut method. Furthermore, the present method provides single-particle wave functions of subsystems, which are useful in the microscopic analysis of structures of subsystems, and is applicable to the study of structural changes of subsystems in cluster structures and nuclear reactions, depending on the internuclear distance. In the applications involving AMD wave functions of $J^\pi = 0_1^+$ and 0_2^+ states in ^{10}Be , although the existence of clusters was not assumed, the proposed method was proven to be useful in the separation of ^{10}Be wave functions into subsystems α and ^6He , when the neck positions and the single-particle orbits (Fig 8) are compared. The proposed method is applicable to the separation of Slater determinant wave functions with neck structures into spatially localized subsystems.

As mentioned above, the present method gives wave functions of subsystems with which expected values of operators can be calculated. For example, the calculation of mass centers of subsystems determines the internuclear distances of $\alpha + \alpha$, $\alpha +$

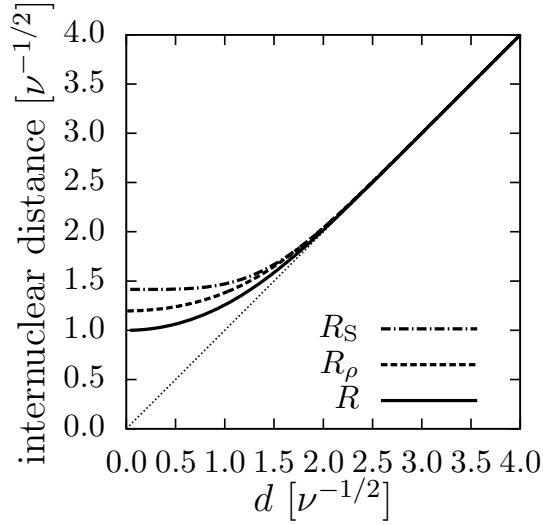


Fig. 9. Internuclear distance for the $\alpha + \alpha$ MB wave functions specified by the parameter d . The distance R defined in the present method and R_ρ defined by the sharp-cut density are plotted. The distance R_S defined by Saraceno et al. is also shown. Units are in $\nu^{-1/2}$

^{16}O , and $^{16}\text{O} + ^{16}\text{O}$ systems, as shown in Figs 3, 5, and 7, respectively. The present method is useful in the study of cluster structures and nuclear reactions because the internuclear distance is an important degree of freedom in these phenomena.

For an $\alpha + \alpha$ system, Saraceno et al. proposed another definition of the internuclear distance,⁶⁾

$$R_S = \sqrt{\frac{1 + e^{-\nu d^2}}{1 - e^{-\nu d^2}}} d = \sqrt{1 + e^{-\nu d^2}} R. \quad (4.1)$$

The form of R in the present definition resembles that of R_S in the denominator, but is smaller than R_S because of the factor $\sqrt{1 + e^{-\nu d^2}}$ (Fig. 9), and in the $d = 0$ limit, $R = R_S/\sqrt{2}$. In the present method, single-particle orbits are assumed to be completely orthogonal. Under this condition, the internuclear distance is smaller than R_S . With the increase in d , both the distances R and R_S approach d .

§5. Conclusions

In this paper, we proposed a method to separate a Slater determinant wave function with a neck structure into spatially localized subsystems. Our method is applied to the MB wave functions of $\alpha + \alpha$, $\alpha + ^{16}\text{O}$, and $^{16}\text{O} + ^{16}\text{O}$ systems, and the AMD wave functions of the $J^\pi = 0_1^+$ and 0_2^+ states in ^{10}Be .

The proposed method obtains wave functions of subsystems with no singularity, which is an advantage over the sharp-cut method. Using the obtained subsystem wave functions, we calculated the expected values of operators for subsystems. For example, the internuclear distance is well defined by the calculated mass centers of the subsystems.

The proposed method is simple and applicable to a wide variety of approaches

that are based on the Slater determinant wave function, e.g., the HF method. It is useful for the analysis of systems that have spatially localized subsystems in phenomena such as cluster structures and nuclear reactions.

Acknowledgments

Numerical calculations were conducted on the high-performance computing system in the Research Center for Nuclear Physics, Osaka University. The authors thank Prof. H. Horiuchi and Dr. M. Kimura for fruitful discussions and valuable comments. This work was supported by the KAKENHI(C) 22540275.

References

- 1) A. Ono, H. Horiuchi, T. Maruyama, and A. Ohnishi, Phys. Rev. Lett. **68** (1992), 2898.
- 2) A. Ono, H. Horiuchi, T. Maruyama, and A. Ohnishi, Prog. Theor. Phys. **87** (1992), 1185.
- 3) Y. Kanada-En'yo and H. Horiuchi, Prog. Theor. Phys. **93** (1995), 115.
- 4) H. Margenau, Phys. Rev. C **59** (1941), 37.
- 5) Y. Kanada-En'yo, H. Horiuchi, and A. Dote, Phys. Rev. C **60** (1999), 064304.
- 6) M. Saraceno, P. Kramer, and F. Fernandez, Nucl. Phys. A **405** (1983), 88.